Proceedings of ALGORITMY 2012
pp. 362–370

GEOMETRIC PROPERTIES OF PARTICLE ENSEMBLES IN TERMS OF THEIR SET COVARIANCE

WILFRIED GILLE*

Abstract. The set covariance $C(r)$ is a basic function in stochastic geometry,frequently applied in the field of image analysis. On the other hand, $C(r)$ is interrelated to the real space structure functions defined in the field of small-angle-scattering (SAS). Fundamental results of stochastic geometry can be transformed to the field of SAS. By use of integral transformation, scattering data of sample materials lead to the real space structure functions. These functions reflect specific geometric properties of the sample material.
Let the order range of a sample be denoted by L. Let $\gamma = \gamma(r)$, $0 \le r \le L$, $\gamma(r) \equiv 0$ if $L < r$, be the SAS correlation function of an isotropic two-phase ensemble of homogeneous, hard particles of volume fraction c. Then, $\gamma(r) = [C(r)/c - c]/(1-c)$. It is shown that the first zero point $\gamma(r_1) = 0$, $0 < r_1 \le L$, can be traced back to four terms: To c of the particles, to a term $\gamma_0(r_1)$ involving the correlation function $\gamma_0(r)$ of the isolated single particle, to a term P_{AB} (second order particle shape specific probability) and to the particle to particle pair correlation function $g(r)$. The obtained formula (a quasi-diluted particle ensemble represents a special case) is exemplified for the model correlation function of a *Dead Leaves model* and for selected experimental cases.

Key words. set covariance, SAS-correlation function, pair correlation, dead leaves model

AMS subject classifications. 65C50, 42A38, 52A22, 53C65

1. Introduction.

In small-angle scattering (SAS), the intensity scattered by a sample is recorded as depending on the scattering vector. Scattering experiments of isotropic sample materials yield isotropic scattering patterns $I = I(h)$, where h denotes the amount of the scattering vector. The SAS correlation function (CF) $\gamma = \gamma(r)$ is a basic structure function for real space data interpretation of a large class of scattering experiments. Fourier transformation of $I(h)$ yields $\gamma(r)$, [1],

$$\gamma(r) = \int_0^L h^2 I(h) \cdot \sin(hr)/(hr) dh \Big/ \int_0^L h^2 I(h) dh.$$

For a specific sample, the order range L is an important input parameter. Compared with the field of image analysis, SAS does not start from image material of a sample for an L. However, based on $I(h)$ of a particle ensemble, see [2], the function γ is compared with geometric models, described by specific model parameters. The particle volume fraction c always belongs to the set of such parameters. Let n be the number of hard particles per volume unit and V_0 the mean particle volume. Then, $c = n \cdot V_0$. In fact, based on $\gamma(r)$, c of isotropic random two-phase systems can be determined from a relative measurement of $I(h)$.
Based on these approaches, it is an experimentally established fact that $\gamma(r)$ involves one or more zero points $r = r_1$, $r = r_2, ...$, see Figs. 1.1 and 1.2. The theoretical background of the first zero point $r = r_1$ will be analyzed here. The investigation and interpretation of this first zero for a random two-phase system has been a long-standing problem in stochastic geometry and SAS. A lot of geometric parameters influence the zero points $r = r_i$. An interpretation of the equation $r = r_1$ will be given in this article.
After a theoretical part, (2.4) will be a main result, followed by applications. Three types

*Martin-Luther-University Halle-Wittenberg, Institute of Physics, D-06120 Halle, Germany, (gille@physik.uni-halle.de)

of particle ensembles of nanometric particles, occurring in materials research, have been selected: First, a test with simulated data of a Dead Leaves model (DLm) is explained. Data recorded in SAS-laboratory by the author on VYCOR glass with CuK_α-radiation are analyzed in section 3. Furthermore, data of convex particles from international SAS conferences measured by use of synchrotron radiation are discussed. For equally sized hemispheres, the particle to particle correlation is discussed in section 4.

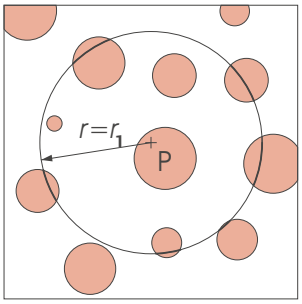

FIG. 1.1. *Interpretation of the first zero of the CF, see Fig. 1.2 in a plane section: The random test point P in a particle is the center of a circle of radius $r = r_1$. The area fraction c equals to [the mean total length of the boldly drawn parts of the perimeter] over $[2\pi r_1]$. In the spatial case, parts of surface areas are operated with. Then, the denominator term is $(4\pi r_1^2)$.*

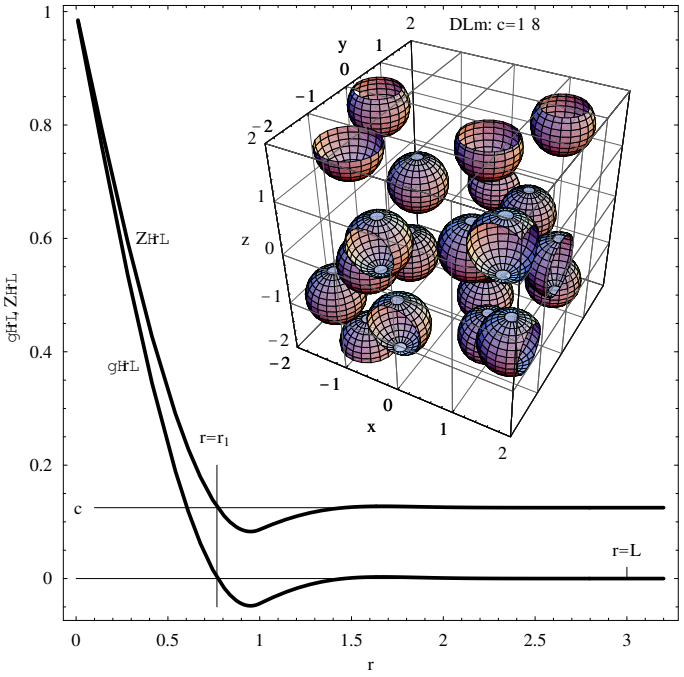

FIG. 1.2. *The functions $\gamma(r)$ and $Z(r) = C(r)/c$ for a Dead leaves model, i.e. for a simulated ensemble of spheres. Overlapping and touching of the particles are not possible. For the interpretation of the length r_1 in the equation $\gamma(r_1) = 0$, see Fig. 1.1. Based on (2.1), $Z(r_1) = c$.*

2. Basic equations for random two-phase systems of hard, convex particles. As a two-phase particles system may involve several order ranges L_i, a well-defined L must be specified [3]. Based on $I(h)$, the sample CF $\gamma = \gamma(r, L)$ results via a Fourier transformation of band limited data. The relation $\gamma(r, L) \equiv 0$, if $L < r$, is incorporated into well-tested computer programs for such integral transformations. For the sample CF, the abbreviations $\gamma(r)$ or γ are used instead of $\gamma(r, L)$.
The CF is the convolution square of the (electron) density fluctuation of the sample. Starting from a diluted system of hard particles, the electron density fluctuation increases with increasing particle number per sample volume. So, $\gamma(r)$ will possess negative values, $-c/(1-c) < \gamma(r) < 0$, at certain abscissas r, $0 \leq r_1 < r$, see Fig. 1.2. To illustrate this in detail, a plane section is considered in Fig. 1. An ensemble of equally sized spheres, possessing a well-defined volume fraction c, is intersected by a plane.
A random point P (the center of a circle of radius r_1) is uniformly distributed in each particle. If $r = r_1$, then the mean length ratio, *[sum of the boldly-drawn parts of the perimeter]* over *[the whole circle perimeter]* equals c, see (2.1). This deliberation is a special case of Rosiwal's linear integration principle, see [4]. Fig. 1.2 involves a three-dimensional simulation. The same will be argued in connection with the later micrograph, see Fig. 3.2.

As early as in 1951, the physicist Porod [1] established a fundamental relationship between the particle volume fraction c, $0 \leq c < 1$, and the SAS structure functions $Z(r)$ (the so-called function of occupancy) and $\gamma(r)$,

$$Z(r) = (1 - c) \cdot \gamma(r) + c. \tag{2.1}$$

The properties $Z(0) = 1$ and $Z(\infty) = c$ are fulfilled. Furthermore, (2.1) yields $c = Z(r_1)$. This special case connects $\gamma(r_1)$, $Z(r_1)$, r_1 and c. The probability $Z(r)$ is connected with the isotropized set covariance $C(r)$ of the particle system via $C(r) = c \cdot Z(r)$, see [4].
If there are only a few small particles embedded in a large homogeneous sample volume, then $c \to 0$ and $Z(r) \approx \gamma(r)$, see (2.1). In such a case, the length L has large values (sometimes undetectable by use of SAS experiments). Then, zeros $\gamma(r_i) = 0$ exist at relatively large lengths r_i. Larger volume fractions, say $c > 0.2$, lead to smaller r_i, if all the other parameters remain constant. Furthermore, there is the special case of the so-called quasi-diluted particle system, see Fig. 2.1.
In the following section, the general case described by (2.1), without any restrictions to the particle to particle distances, is considered. These distances are characterized by the *particle to particle (pair) correlation function* $g(r)$. The connection of these parameters with the first zero $r = r_1$ of the CF will be investigated in detail in the next subsections.

2.1. A basic equation for the function $\gamma = \gamma(r, L)$. The length r_1 is closely interrelated with the function $g(r)$ of the single particles. Let these single particles possess a mean correlation function $\gamma_0(r)$. Then, see [5],

$$\gamma(r) = \frac{1}{1-c} \cdot \left(\gamma_0(r) - c + \frac{c}{V_0} \cdot \int_0^L 4\pi l^2 g(l) \cdot P_{AB}(r, l) dl \right). \tag{2.2}$$

Here, V_0 denotes the single particle volume, and the function $P_{AB}(r, l)$ in the integrand represents a special geometric probability, depending on size and shape of the particles: the probability of finding two points placed in two single particles of maximum diameter L_0, whose centers are separated by a distance l.
In detail, for $L = L_0$ the term $P_{AB}(r, l)$ defines the following: For two single particles A and B, whose centers are separated by a distance l, $L_0 \leq l$, the function $P_{AB}(r, l, L_0)$ is the geometric probability that a point X_B which is placed at a fixed distance r from a point X_A in A is in particle B. Analytic expressions of P_{AB} have been established for spheres [4]. The integration limits of the integral in (2.2) have to reflect all possible minimum and maximum distances between all pairs of particles A and B. In the special case $c = 0$ - independent of

the functions $g(r)$ and $P_{AB}(r,l)$ and of the integration limits - $\gamma = \gamma_0$ results. All terms involved in (2.2) have been checked and applied in experimental cases [5] and [6]. This implies that the interpretation of the zero-case $\gamma(r_1) = 0$ is not a trivial problem, because several geometric parameters are closely interrelated.

In practice, the volume fraction c is always connected with an order range L of the particle arrangement [3]. It is indispensable to fix a selected L in order to obtain the scattering pattern, impacted by the parameters L, c, γ_0, V_0, g and P_{AB}.

2.2. Interpretation of the first zero of the sample correlation function, $r = r_1$. The order relation $0 \le c < 1$ must be fulfilled, as a complete filling of the space with particles (if possible at all) contradicts the assumption of an isotropic sample. In the case $\gamma(r_1) = 0$, it follows from (2.1)

$$0 \equiv \gamma_0(r_1) - c + \frac{c}{V_0} \cdot \int_0^\infty 4\pi l^2 g(l) \cdot P_{AB}(r_1, l) dl. \tag{2.3}$$

Thus, c is explicitly defined in terms of r_1, γ_0, V_0, g and P_{AB},

$$c = \frac{\gamma_0(r_1)}{1 - \frac{1}{V_0} \cdot \int_0^\infty 4\pi l^2 g(l) \cdot P_{AB}(r_1, l) dl}. \tag{2.4}$$

Equation (2.4) is an essential result. Several parameters are interrelated. A more simple equation could hardly be expected. In the following, special cases for the parameters involved in (2.4) will be analyzed. Taking into account a largest particle diameter L_0, the particle volume V_0 results from $V_0 = \int_0^{L_0} 4\pi r^2 \gamma_0(r) dr$.
The connection (2.4) can be verified by a numerical calculation for a Dead Leaves model (DLm) with spherical primary grains of constant diameter d, Fig. 1.2. Assuming a sphere diameter $d = L_0 = 1$, the numerical calculation yields $r_1 = 0.768 \cdot d$. In detail, $\gamma_0(r_1) = 0.075$ results. After inserting all parameters into (2.4), the theoretically expected value $c = 1/8$ results [7].
Of course, (2.4) remains valid in the special case $c \to 0$. This is closely connected with the single particle CF $\gamma_0(r)$, which disappears if $L_0 \le r < \infty$. The denominator term of (2.4) equals 1, because the integral term disappears. The only one zero of the CF is given by $\gamma_0(L_0) = 0$. Thus, in this limiting case, $r_1 = L_0$ follows. Consequently, $c = \gamma_0(L_0)/(1 - 0/V_0) \equiv 0$ results.
Furthermore, (2.4) fulfills the case of a quasi-diluted particle arrangement analyzed in the next subsection.

2.3. Quasi-diluted particle ensembles. This interesting special case of the particle to particle interaction results if the smallest chord length between any two particles $l_m = \min(l_i)$ is larger than the maximum diameter of the largest particle $L_0 = \max(L_i)$. A case with three different particles is illustrated in Fig. 2.1, $\max(L_i) < \min(l_i)$.
Here, $g(l) = 0$ if $0 \le l < L_0 + l_m$. Now, taking into account $r_1 \le L_0 + l_m$, the integral term

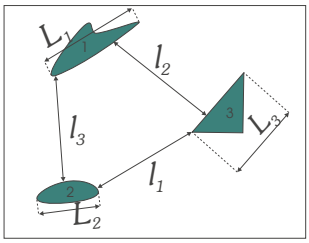

FIG. 2.1. *Exemplification of a quasi-diluted particle arrangement for three particles.*

$T(r)$ in (2.4),

$$T(r) = \int_{L_0+l_m}^{\infty} 4\pi l^2 \cdot g(l) \cdot P_{AB}(r,l)dl, \tag{2.5}$$

disappears at $r = r_1$. It follows $T(r_1) = 0$. On the other hand, indeed $\gamma(r) = \gamma_0(r)$, if $0 \le r \le L_0$. Operating with the zero of $\gamma(r)$ at $r = r_1$, $\gamma_0(r_1) = c$ follows from (2.2). Inserting these special results into (2.4), $c = \gamma_0(r_1)/(1 - 0/V_0) = \gamma_0(r_1)$ is obtained.

3. Application in experimental cases. In the following, two independent practical applications are explained. While the first one is based on an author measurement in the SAS laboratory at the university of Halle with CuK_α–radiation [19], the second one was performed in Grenoble by other scientists with synchrotron radiation [14, 15], at a time when the author was theoretically establishing the fundamentals of (2.4).

3.1. VYCOR glass data. Based on the scattering pattern of a VYCOR glass of type 7930 sample [3], an ideal isotropic two-phase sample, the function $\gamma(r)$ has been obtained, Fig. 3.1. Assuming long, nearly cylindrical pores in an isotropic uniform random spatial arrangement, after intermediate calculations for $L = 30\ nm$ with $r_1 = 8\ nm$, (2.4) yield the volume fraction $c = 0.35$. This result is in agreement with the results obtained by two other experimental methods, namely: nitrogen adsorption, mercury intrusion and additionally from the theoretical approach based on the density of the components of this glass, (for more details see figure 4 in [3]).

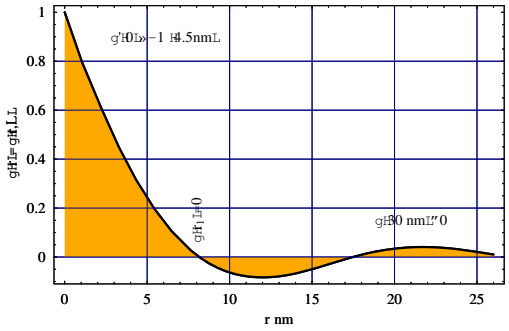

FIG. 3.1. *The SAS CF of VYCOR–7930 glass: Based on $L = 30\ nm$, the first zero of the SAS CF is at $r = r_1 = 8\ nm$. The second zero, $r = r_2 \approx 18\ nm$, is not discussed.*

3.2. Ni-base alloy. Based on scattering experiments, performed at the Microfocus beamline (ID13) of the European Synchotron Radiation Facility in Grenoble in 2001/2004, tightly packed phases of a Ni-base alloy have been investigated [13], see the micrograph Fig. 3.2. For explaining the approach used see Fig. 1.1, and furthermore, for explaining the concept of chord length distributions [16, 17, 20] in detail an original micrograph, see [14], has been supplemented: The modification shows a straight test line with chord segments l_i and m_i and several test circles with the radius $r = r_1 = 40\ nm$.
Some remarks are useful: Based on a direct analysis of Fig. 3.2, considered as a planar section, the particle phase volume fraction is expected to be smaller than 70%. However, due to the preparation procedure for obtaining the micrograph, the surface regions have been modified. There exists a dilution of particle density near the surface area, at least up to a depth of $t < 0.3\ \mu m$. Thus, the micrograph is far from being a plane section.

From the recorded scattering curve of the alloy [15], an SAS CF possessing a clear negative region starting with the zero at $r_1 = 40\ nm$ results, Fig. 3.3. Here, $L = 150\ nm$, which means that a micrograph of edge lengths (150 nm × 150 nm) involves all the geometric information about the spatial arrangement of the γ'-cubes. The whole particle system can be approximated by a tightly packed isotropic cube model (nearly constant particle sizes),

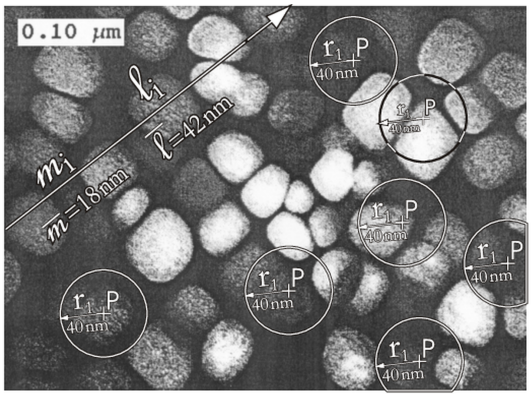

FIG. 3.2. *Micrograph illustrating the local microstructure of a W-rich Ni-base γ/γ'-alloy [14, 15, 18]: The shape of the γ'-particles can be approximated by parallelepipeds.*

possessing a volume fraction $c = c(L)$. Based on the theory presented, via (2.4) a volume fraction of the particle phase $c = c(L) = 0.7$ follows and for the matrix $1 - c(L) = 0.3$.
These results are in agreement with other stereological parameters, that result from Figs. 3.2 and 3.3: The mean chord length inside the cubes equals $\bar{l} = 42\ nm$ and that of the intermediate spaces is $\overline{m} \approx 18\ nm$. Together with the first derivative $\gamma'(0) = -1/(13\ nm)$, these parameters fulfill the equation $|\gamma'(0)| = 1/\bar{l} + 1/\overline{m}$ and agree with a stereological analysis of the micrograph Fig. 3.2. The pair correlation can be approximated by the parameter model described by Thiele [6], see also section 4.1. and Fig. 3 in [3].
Altogether, approximating the particle shape by the cube model, inserting the minimum edge length of the γ' particles $a_{min} = 50\ nm$ and assuming an isotropic uniform random arrangement, a volume fraction of the particle phase $c = c(L) = 0.7$ is obtained via this interpretation of the CF.

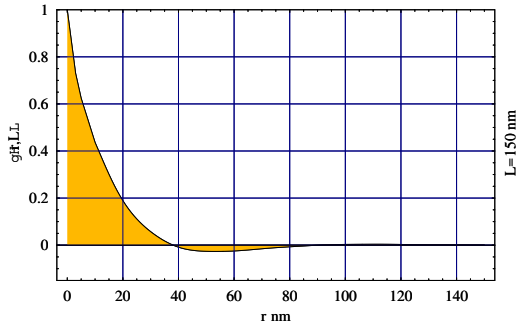

FIG. 3.3. *The SAS CF function possesses a zero at $r = r_1 = 40\ nm$ and reflects details of the geometry of the γ'-phase.*

4. About the function $P_{AB}(r, l)$. The interpretation of the applications given is mainly based on the introduction of the function P_{AB} in (2.2). More details about this function are explained now.
The probability P_{AB} describes the essential part of the particle to particle correlation. This is a second order particle to particle correlation function, which - in the general case - includes a combined translation and rotation of two particles A and B.
A fixed position of A and B is considered. Inside B there is a certain part $S(r)$ of the surface

area $4\pi r^2$ of the *sampling sphere* of radius r centered at point P in the particle A. For the elementary plane case see Fig. 1.1. The term P_{AB} is given by the averaged second order particle to particle overlapping

$$P_{AB}(r) = \frac{\overline{S(r, l, \vartheta_1, \phi_1, \vartheta_2, \phi_2)}}{4\pi r^2}. \tag{4.1}$$

In contrast to the first order particle correlation, here the determination of the probability P_{AB} requires a mutual rotation of the particles A and B. For each constant r, four direction angles ϑ_1, ϕ_1, ϑ_2, ϕ_2 define the positions of A and B in space.
This equation can be handled numerically for any particle shape, even if A and B differ in size and shape. This requires the analysis of a sequence of $g_{ij}(r)$ pair correlation functions, describing the distances between the corresponding particles of certain shapes A_i and B_j.

It follows an example of utilization for hemispheres of diameter d, possessing an isotropic uniform random spatial orientation:
Here, $P_{AB}(r, l, d)$ is given by

$$P_{AB}(r, l, d) = \frac{1}{2} \cdot \int_0^{\vartheta_o} \gamma_0\big(\sqrt{r^2 + l^2 - 2r \cdot l \cdot \cos(\vartheta)},\ d\big) \cdot \sin(\vartheta) d\vartheta. \tag{4.2}$$

The upper integration limit $\vartheta_o = \vartheta_o(r, l, d)$ defines the real volume overlapping, if the integrand possesses positive real values. Thus, the probability P_{AB} is traced back to the CF $\gamma_0(r, d)$ of a single hemisphere [10]. The upper integration limit in (4.2) is defined by the geometric overlapping conditions between the particles A and B. Based on (4.2) and (4.3), P_{AB} has been obtained [11], operating with the isotropized normalized CF of a hemisphere $\gamma = \gamma_0(r, d)$, see the following *Mathematica* expression,

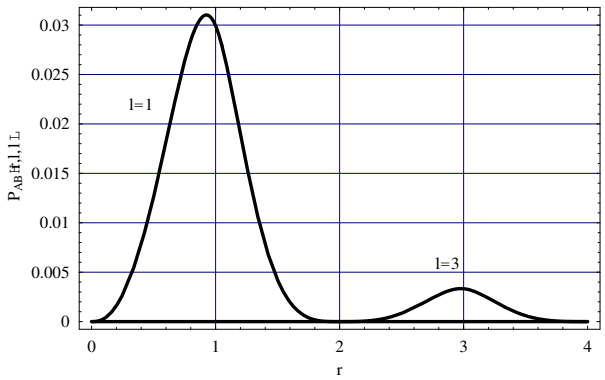

FIG. 4.1. *The function $P_{AB}(r, l, d)$ for hemispheres with $d = 1$: Two different particle to particle distances l, $l = 1$ and $l = 3$, have been inserted.*

$$\begin{aligned}
\gamma[r_, d_] = {} & Which\big[0 \le r \le \frac{d}{2}, 1 - \frac{9r}{4d} + \frac{r^3}{d^3} + \frac{3\big(r^2 - \frac{d^2}{4}\big)\sin^{-1}\big(\frac{r}{d}\big)}{2\pi r d}, True, 0\big] \\
& + Which\big[\frac{d}{2} \le r \le d, \frac{3\big(\frac{d^2}{4} - r^2\big)\cos^{-1}\big(\frac{r}{d}\big)}{2\pi r d}, True, 0\big] \\
& + Which\big[0 \le r \le d, \frac{3\big(\frac{2d^2}{4} + r^2\big)\sqrt{d^2 - r^2}}{4\pi d^3}, True, 0\big].
\end{aligned} \tag{4.3}$$

Two special probability cases, $P_{AB}(r, 1, 1)$ and $P_{AB}(r, 3, 1)$, have been analyzed in Fig. 4.1. If $d \ll l$, the maximum $max[P_{AB}(r, l, d)]$ exists at $r \approx l$. The exact agreement $r = l$ results

in the limiting case $l \to \infty$. Based on $P_{AB}(r, l, d)$, see Fig. 4.1, the scattering pattern $I(h)$ of an isotropic arrangement of hemispheres is defined based on (2.2).

5. Discussion and conclusions. In a way, the data analysis of a scattering pattern via its sample CF can be compared with the stereological analysis of image material (image processing). Of course, the latter is a more direct approach, whereas the interpretation of the SAS CF requires more assumptions (isotropy, two-phase system, mainly hard, convex particles/pores, specific order range L) compared with image processing. For this it is clear that the assumption of a specific L is indirectly also involved in each procedure of image processing: Each actual image automatically involves a specific L, given by the fixed magnification of an image (micrograph).

The volume fraction $c = c(L)$ (i.e., in the case of porous materials, the porosity) is reflected in the behavior of all SAS structure functions: On the one hand, there are methods mainly based on an absolute measurement of the scattering intensity $I(h)$. Furthermore, there exists another group of methods, based on relative intensity measurement. This article adds a further approach to the latter group. The volume fraction of hard particles is explicitly given by (2.4), where r_1 is a deciding experimental parameter. Thus, the new connection (2.4) joins the sequence of existing approaches for determining the volume fraction of two-phase systems via scattering experiments. It would be interesting to compare all these methods and discuss advantages and disadvantages. However, this would require an essentially longer paper.

Contrary to the pure chord length analysis [2], Rosiwals's linear integration principle, which has been modified by a method mainly based on $\gamma'(0)$, see [3], and the considerations performed in [5] for non-convex particles and [16] and the papers [17]–[20], here the pair correlation function $g(r)$ is directly included. The geometric probability $P_{AB}(r, l)$, which can be determined for the existing particle shape in question, traces the determination of c back to the pair correlation between two particles.

The interpretation of the first zero of the SAS CF proves to be a complex matter. So, the length $r = r_1$ is a characteristic parameter of the SAS CF. The length r_1 is influenced by the whole geometry of the particle arrangement, the single particles and their spatial arrangement.

Mainly based on the parameter r_1, but with additional information, it is possible to estimate the particle volume fraction c. Here, besides the pair correlation $g(r)$ a certain function P_{AB} is involved. In the case of spherical particles, there exists a simple analytic representation of P_{AB}. For other particle shapes, like hemispheres, tetrahedrons, circular cylinders, parallelepipeds and right circular cones, P_{AB} can be obtained numerically, see the example given by (4.3) and Fig. 4.1.

The examples demonstrate that the approach can be used for determining the volume fraction of two-phase materials if the particle shape is known a priori.

Acknowledgments. The author thanks the reviewer very much for the report. Taking into account all the useful hints, the author comes to the inclusion that these results really can be arranged (belong) to the topic *image processing* of the conference. This holds true, although the actual paper does not start from any image material at all.

REFERENCES

[1] G. Porod, *Die Roentgenkleinwinkelstreuung von dichtgepackten kolloiden Systemen*, Kolloid Zeitschrift, 124 (1951), pp. 83–114.

[2] W. Gille, *Chord length distributions and small-angle scattering*, The European Physical Journal B, 17 (2000), pp. 371–383.

[3] W. Gille, *Volume fraction of random two-phase systems for a certain fixed order range from the SAS correlation function*, Mat. Chem. & Phys., 77 (2002), pp. 612–619.

[4] D. Stoyan, W. S. Kendall and F. Mecke, *Stochastic geometry and its applications*, Second ed., Akademie Verlag, Berlin, 1990.

[5] W. Gille, *Volume fraction of hard particles from small-angle scattering experiments*, Comp. Mat. Sci., 25 (2002), pp. 469–477.

[6] E. Thiele, *Equation of State for Hard Spheres*, J. Chem. Phys., 19 (1963), pp. 474–479.

[7] D. Stoyan and M. Schlather, *Random sequential adsorption: relationship to dead leaves and characterization of variability*, J. Statist. Phys., 100 (2000), pp. 969–979.

[8] S. Ciccariello, *Integral expressions of the derivatives of the small-angle scattering correlation function*, J. Math. Phys., 26 (1995), pp. 219–246.

[9] W. Gille and M. Kraus, *Geometric parameters of isotropic ensembles of right cylinders from the SAS correlation function*, Acta Cryst. A, (2010), pp. 597–601.

[10] W. Gille, *The small-angle scattering correlation function of the hemisphere*, Comp. Mater. Sci., 15 (1999), pp. 449–454.

[11] Wolfram Research, *Inc., Mathematica*, version 7.01., Champaign, Illinois, 2003.

[12] L. A. Feigin and D. I. Svergun, *Structure Analysis by Small-Angle X-ray and Neutron Scattering*, Plenum, New York, 1987.

[13] S. V. Roth, M. Burghammer, R. Gilles, D. Mukherji, J. Rsler and P. Strunz, *Precipitate scanning in Ni-base-super-alloys*, Nuclear Instruments and Methods in Physics Research B, 200 (2003), pp. 255–260.

[14] S. V. Roth et al., *Precipitate scanning in Ni-base-super-alloys*, Contribution: International Conference on Small-Angle Scattering, Venezia, 2002.

[15] R. Gilles, *Private communication*, Poster session: International Conference on Small-Angle Scattering, Venezia, 2002.

[16] W. Gille and A. Brown, *SAXS chord length distribution analysis and porosity estimation of activated and non-activated glassy carbon*, J. of Non-Crystalline Solids, 321 (2003), pp. 89–95.

[17] W. Gille, D. Enke, F. Janowski and T. Hahn, *About the Realistic Porosity of Porous Glasses*, J. of Porous Materials, 10 (2003), pp. 179–187.

[18] M. Durand-Charre, *The Microstructure of Superalloys*, Gordon and Breach, Singapore, 1997.

[19] W. Gille, D. Enke and F. Janowski, *Pore Size Distribution and Chord Length Distribution of Porous VYCOR Glass*, J. of Porous Materials, 9 (2002), pp. 221–239.

[20] W. Gille, *Cross-section structure functions in terms of the three-dimensional structure functions of infinitely long cylinders*, Powder Technology, 138 (2003), pp. 124–131.